



ELSEVIER

Available online at www.sciencedirect.com

SCIENCE @ DIRECT®

Surface Science 521 (2002) L669–L673



www.elsevier.com/locate/susc

Surface Science Letters

Crossover between terrace-diffusion and diffusion step-to-step on vicinal surfaces: scaling function and analytic approximations

T.L. Einstein *

Department of Physics, University of Maryland, College Park, MD 20742-4111, USA

Received 18 June 2002; accepted for publication 2 August 2002

Abstract

On equilibrium vicinal surfaces with mass transport dominated by terrace-diffusion (TD), there can be crossover from TD to diffusion step-to-step (DSS) behavior for fluctuation wavelength λ large compared to the step separation ℓ . We show that the temporal correlation function for 180°-out-of-phase fluctuations can be written as a function of a single dimensionless variable proportional to time/ℓ^3 and present an excellent, simple approximation for this scaling function. This formulation can be used to distinguish mass transport dominated by DSS versus evaporation–condensation (attachment–detachment) limited kinetics (for which the capillary-wave characteristic time τ has the same λ^2 behavior as DSS).

© 2002 Elsevier Science B.V. All rights reserved.

PACS: 5.40.-a; 68.35.-p; 68.37.-d; 5.70.Np

Keywords: Vicinal single crystal surfaces; Models of surface kinetics; Equilibrium thermodynamics and statistical mechanics; Surface diffusion

The temporal correlation function for equilibrium fluctuations of isolated steps has received a great deal of analytical attention and has been rather thoroughly described [1–4]. It is well established that a capillary wave analysis can be used to distinguish the three limiting cases by examining the wave vector dependence of the time constant characterizing the healing of fluctuations: $\tau_q^{-1} \propto q^2$, q^3 , or q^4 , for evaporation–condensation (EC),

terrace-diffusion (TD), or periphery-diffusion (PD) limited transport, respectively. (Here $q \equiv 2\pi/\lambda$ is the wave vector of the step fluctuation.) On a vicinal surface, other behaviors also become possible [1,5]. The crossover between these various limits is a subject of active interest. For instance, and of specific concern in this paper, Pimpinelli et al. [5] argued very generally that TD-dominated vicinal surfaces should crossover from TD into diffusion-step-to-step (DSS) behavior at small q (i.e. $q\ell < 1$, where ℓ is the mean step separation); operationally, one of the q 's in τ_q^{-1} is supplanted by $1/\ell$, leading to q^2/ℓ behavior. While TD behavior

* Tel.: +1-301-405-6147; fax: +1-301-314-9465.

E-mail address: einstein@physics.umd.edu (T.L. Einstein).

is easy to achieve in numerical simulations [7], it has not to date (with the notable exception of Cu(111) in HCl [8]) been seen in experiments [9,10]. Moreover, to properly interpret the pre-factor of q^2 seen in such measurements, it is crucial to know whether the underlying mechanism is EC or DSS. Note that, for simplicity, we assume here that diffusion along the step edge is negligible.

For “pure” cases in which $\tau_q^{-1} = A_n q^n$, the temporal autocorrelation function $G_n(t)$ (or, equivalently, the mean-square width $w^2(t/2)$ of the step fluctuations [3,4]) has been shown in several papers to satisfy the following equation, arising from a capillary wave analysis:

$$\begin{aligned} G_n(t) &\equiv \langle [x(t+t') - x(t')]^2 \rangle_{t'} \\ &= (2k_B T / \pi \tilde{\beta}) \int_0^\infty dq q^{-2} [1 - \exp(-t A_n q^n)] \\ &= (2k_B T / \pi \tilde{\beta}) (t A_n)^{1/n} \Gamma(1 - 1/n). \end{aligned} \quad (1)$$

We focus on the case $n = 3$, which for an isolated step corresponds to TD limited fluctuations; in this case, $A_3 = 2\tilde{\beta}\Omega^2 c_t D_t / k_B T$, where $\tilde{\beta}$ is the step stiffness, Ω the atomic area, $c_t D_t$ the product of terrace atom (or vacancy) concentration and diffusion constant, and $k_B T$ the thermal energy. Eq. (1) becomes $G_3(t) = (2k_B T / \pi \tilde{\beta}) \Gamma(2/3) A_3^{1/3} t^{1/3}$.

A more detailed treatment of the crossover between TD and DSS was given in Ref. [1]. In addition to decomposing fluctuations into capillary modes along each step, one must consider the relative phases of these modes on all the steps on the vicinal surface. In principle, as in Ref. [6], one can consider an arbitrary phase angle Φ between adjacent steps, writing

$$x_\Phi(y, t) \equiv M^{-1} \sum_m e^{-im\Phi} x_m(y, t), \quad (2)$$

where m indexes the large number (in principle infinite) M of steps. Following Ref. [1] we just consider symmetric ($\Phi = 0$, phase factor 1, called Σ in [1]) and fully out-of-phase, antisymmetric ($\Phi = \pi$, phase factor -1 , called Δ in [1]) modes. As shown in Ref. [1], the Σ decomposition has idiosyncratic behavior with $\tau_q^{-1} \propto q^4$ in the DSS regime, while the Δ decomposition has the expected q^2 behavior which presumably characterizes arbitrary phase angle. Hence, we focus here on the latter case. To

characterize behavior for arbitrary value of $q\ell$, the integer exponent n of q should be replaced by a continuously variable exponent z_q . For the case of insignificant Ehrlich–Schwoebel asymmetry and $qd \ll 1$, where d is the “kinetic” length [11] (so setting $a_q \equiv qd = 0$ in Eq. (54) of Ref. [1]),

$$z_q = 3 - q\ell / \sinh(q\ell), \quad (3)$$

which is 3 for large values of $q\ell$ and drops smoothly but relatively abruptly to 2 for small $q\ell$. However, that paper did not pursue the consequences in real space. Since measurements are now being made [10,12] which need to distinguish between EC and DSS behavior, it is timely to present some formal results which should be helpful in analyzing data. (Explicit, albeit preliminary, Monte Carlo studies of the crossover [13] have also been reported.) In this short communication, we point out scaling behavior that the correlation function should exhibit in DSS and present an exact expression and analytic approximants for the scaling function.

We rewrite Eq. (1) in terms of $x_{\Phi=\pi}$ rather than x and then insert Eq. (3) into it in a manner that maintains proper units, finding

$$\begin{aligned} G_{3 \rightarrow 2}^{(\pi)}(t) &= (2k_B T / \pi \tilde{\beta}) \int_0^\infty dq q^{-2} \\ &\times [1 - \exp\{-t A_3 q^3 / (q\ell)^{q\ell / \sinh(q\ell)}\}]. \end{aligned} \quad (4)$$

It is not hard to carry out numerically the integral in Eq. (4). At early times it goes like $t^{1/3}$, then crosses over to $t^{1/2}$ (over a range of somewhat over a decade in t). To obtain an expression that is more tractable analytically and easier to interpret, we replace $A_3 q^3$ in the argument of the exponential in Eq. (1) by $(A_3/\ell)q^2$ for $q < \varsigma/\ell$, where ς is expected to be of order unity. We then have ¹ a pair of definite integrals, yielding results in terms of the error function and the incomplete gamma function [14]:

$$\begin{aligned} &\int_0^{\varsigma/\ell} \frac{dq}{q^2} \left[1 - \exp\left(-\frac{t A q^2}{\ell}\right) \right] \\ &= -\frac{1 - \exp(-t A \varsigma^2 / \ell^3)}{\varsigma/\ell} + \left(\frac{\pi t A}{\ell}\right)^{1/2} \text{Erf} \left[\varsigma \left(\frac{t A}{\ell^3}\right)^{1/2} \right], \end{aligned} \quad (5a)$$

¹ Note that $\Gamma(1/2, x^2) = \sqrt{\pi}[1 - \text{Erf}(x)]$.

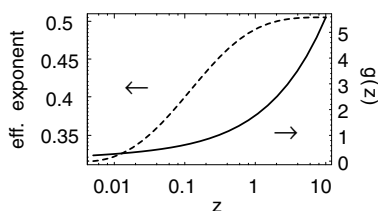


Fig. 1. Plot (solid curve) of the scaling function $g(z)$, where z is the dimensionless time tA_3/ℓ^3 (solid curve, right vertical axis). Also plotted as the dashed curve is the logarithmic derivative of $g(z)$, indicating the effective exponent of $g(z)$ (left vertical axis).

$$\int_{\zeta/\ell}^{\infty} \frac{dq}{q^2} [1 - \exp(-tAq^3)] = \frac{1 - \exp(-tA\zeta^3/\ell^3)}{\zeta/\ell} + (tA)^{1/3} \Gamma\left[\frac{2}{3}, tA\left(\frac{\zeta}{\ell}\right)^3\right]. \quad (5b)$$

Note that for $\zeta \leq 1$, dividing the argument of the exponential by $q\ell$ (due to the replacement of q by $1/\ell$) increases its magnitude, thereby increasing the magnitude of the resulting integral relative to $G_3(t)$. In other words, $G_3(t)$ underestimates the evolution of fluctuation correlations given by $G_{3 \rightarrow 2}^{(\pi)}(t)$, as we shall see again below.

Eq. (4) can be rewritten as a scaling relation involving a function g of the “temporal” dimensionless ratio tA_3/ℓ^3 , containing an integration over the “spatial” dimensionless combination $^2 s \equiv q\ell$:

$$\frac{G_{3 \rightarrow 2}^{(\pi)}(t)}{2k_B T \ell / \pi \beta} = g\left(\frac{tA_3}{\ell^3}\right); \quad g(z) \equiv \int_0^{\infty} ds s^{-2} [1 - \exp(-zs^{3-s} \text{csch}(s))]. \quad (6)$$

(The dimensionless temporal variable z should not be confused with the exponent z_{q^*} .) In Fig. 1 is a plot of $g(z)$ as well as its logarithmic derivative, $d \ln(g(z))/d \ln(z)$. The crossover from $z^{1/3}$ to $z^{1/2}$ evidently occurs between $z \sim 10^{-2}$ and 10^0 . Similarly, the pair of integrals in Eq. (4) can be recast in terms of scaling functions $g_<$ and $g_>$:

² This sort of expression might well have been anticipated since ℓ is the only characteristic length in the direction normal to the steps.

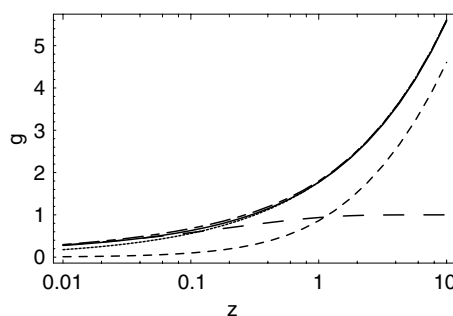


Fig. 2. Comparison of scaling function $g(z)$, as in Fig. 1 and $g_<(z)$ (short dashes), $g_>(z)$ (long dashes), and their sum $g_+(z)$ (long and short dashes). Evidently $g(z)$ is well approximated by $g_<(z) + g_>(z)$. The dotted curve is $(\pi z)^{1/2}$, the result of assuming pure q^2 behavior.

$$g_<(z) \equiv -[1 - \exp(-z)] + (\pi z)^{1/2} \text{Erf}(z^{1/2}), \quad (7a)$$

$$g_>(z) \equiv [1 - \exp(-z)] + z^{1/3} \Gamma(2/3, z). \quad (7b)$$

To leading order in z , $g_<(z) \sim z$ and $g_>(z) \sim \Gamma(2/3)z^{1/3}$. In the other extreme of asymptotic z , $g_<(z) \rightarrow (\pi z)^{1/2}$ and $g_>(z) \rightarrow 1$. These functions are plotted in Fig. 2 along with $g(z)$. Then

$$G_{3 \rightarrow 2}^{(\pi)}(t)/[\ell(2k_B T / \pi \beta)] \cong [g_<(\zeta^2 t A_3 / \ell^3) + g_>(\zeta^3 t A_3 / \ell^3)] / \zeta. \quad (8)$$

Hence, the problem reduces to finding the value of ζ which optimizes by some criterion the correspondence of the trial function $[g_<(\zeta^2 z) + g_>(\zeta^3 z)]/\zeta$ to $g(z)$. The choice adopted here is to optimize the replication of the logarithmic derivative of $g(z)$. In Fig. 3 is a contour plot of ratio of the logarithmic derivative of the trial function to that of $g(z)$: $\zeta^{-1} [d \ln(g_<(\zeta^2 z) + g_>(\zeta^3 z))/dz] / [d \ln(g(z))/dz]$. By this criterion the optimal value of ζ lies between 0.95 and 1.00. Sacrificing a small amount of accuracy for simplicity, we set $\zeta = 1$, so that the $[1 - \exp(-z)]$ terms cancel, giving

$$G_+(t) = \frac{2k_B T \ell}{\pi \beta} \left[\left(\frac{\pi t A_3}{\ell^3}\right)^{1/2} \text{Erf}\left\{\left(\frac{t A_3}{\ell^3}\right)^{1/2}\right\} + \left(\frac{t A_3}{\ell^3}\right)^{1/3} \Gamma\left(\frac{2}{3}, \frac{t A_3}{\ell^3}\right) \right] \quad (9)$$

for our advocated approximation for the DSS-TD crossover function $G_{3 \rightarrow 2}^{(\pi)}(t)$.

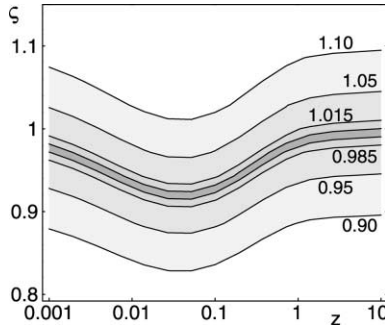


Fig. 3. Contour plot of the ratio of the logarithmic derivative of the trial approximant $([g_<(z^2z) + g_>(z^3z)]/z)$ of the scaling function $g(z)$ to that of $g(z)$ itself, plotted vs. the dimensionless time z and the proportionality constant ζ marking the value of $q = \zeta/\ell$ at which temporal scaling is taken to change abruptly from q^2 to q^3 behavior. The contour lines correspond to labeled values of this ratio; the darker the shading, the closer this ratio is to unity, the ideal value. The darkest region lies between 0.995 and 1.005. Although $\zeta = 1$ is slightly higher than optimal, the analytic convenience makes it a convenient choice. The dips in these contour lines as functions of z correspond to the crossover region.

In Fig. 2 we include a curve for $g_+(z)$, the scaled version of $G_+(t)$:

$$g_+(z) \equiv g_<(z) + g_>(z) = (\pi z)^{1/2} \text{Erf}(z^{1/2}) + z^{1/3} \Gamma(2/3, z). \quad (10)$$

This function exceeds $g(z)$ (the scaled version of $G_{3 \rightarrow 2}^{(\pi)}(t)$) by less than 9% near $z = 0.04$, in the middle of the crossover regime, and the deviation falls rapidly as z enters a “pure” region: $g_+(z)$ is less than 1% greater than $g(z)$ for $z > 2$ or $z < 2 \times 10^{-4}$. Furthermore, approximating $g(z)$ by $g_+(z)$ is notably better than the simplest approximation of using Eq. (1) to estimate $(2k_B T/\pi\beta) \times (tA_n/\ell)^{1/2} \Gamma(1/2)$, i.e. using just $g_2(z) \sim (\pi z)^{1/2}$ instead of $g_+(z)$ [10]. In contrast to $g_+(z)$, $g_2(z)$ is always less than $g(z)$. For large z , the difference between $g_2(z)$ and $g(z)$ is insignificant, but as z decreases, this difference becomes increasingly and insufferably large: by $z = 0.5$, $g_2(z)$ is 1% smaller than $g(z)$; by $z = 0.1$ it is over 10% smaller; by $z = 0.01$ (the smallest value of z displayed in Fig. 2) it is 36% too small, and it continues to fall. For most applications to experiments, use of $g_+(z)$ instead of $g(z)$ should easily be satisfactory, but use

of $g_2(z)$ is questionable unless one knows in advance that z is large.

In the case studied in Ref. [12], which motivated this investigation, the maximum value of z is 5×10^{-3} . Since $g(0.001) = 0.133$, assumption of $t^{1/2}$ behavior for all times and consequent use of g_2 leads to an estimate of z as $0.133^2/\pi$, 5.6 times the true value: assuming all other variables are known, this use of g_2 then produces an estimate of $c_t D_t$ that is 5.6 times the true value. This situation becomes progressively worse at smaller values of z . At $z = 10^{-4}$ or 10^{-5} , e.g., g_2 overestimates by factors of 12.5 or 27.0, respectively. A more stringent test is whether experimental data can be well fit with Eq. (6), using measured values for stiffness and step spacing; for the data in Ref. [12], such was not the case, providing strong evidence that DSS was not the mode of mass transport underlying the step fluctuations.

It was originally recognized [5] that, to distinguish conclusively EC from DSS, one should analyze several values of mean step spacing of a particular vicinal surface. However, use of the scaling formulation in Eq. (6) and the analytic approximation in Eq. (10) are new. To complete the present analysis, an expression for z_q should be constructed that generalizes Eq. (3) to arbitrary values of Φ . Then one should construct approximants to the generalization of Eq. (4) containing an additional integral over Φ (cf. Ref. [6]), with a sufficient number M of steps so that the $\Phi = 0$ mode plays a negligible role.

The approach presented here should be applicable more generally in studying crossover behavior.³ Moreover, observation of data collapse

³ For example, a similar tactic could be used to distinguish TDPS, i.e. TD with a perfect Schwoebel barrier [5], from PD, both of which have $\tau_q^{-1} \propto q^4$. Analogous to Eq. (3), from Eq. (53) of Ref. [1], with the Schwoebel rate asymmetry parameter $r = 0$, we find $z_q = 2 + 2/(1 + q^2 \ell d)$. The crossover behavior is more complicated since the dimensionless combinations $q d$ and $q \ell$ are multiplied. Moreover, as noted in Appendix A of Ref. [1], there is an alternative formalism which is probably more physically realistic and makes a non-trivial difference when both terrace and step-edge diffusion are important. To avoid obscuring the key ideas of this short paper and because TDPS applies only for extreme situations [1], we defer detailed discussion of this example.

by appropriate scaling of independent variables lends confidence to theoretical understanding of the dynamics.

Acknowledgements

This work was supported by NSF MRSEC Grant DMR 00-80008. It grew from a draft appendix to Ref. [12]. I am very grateful to E.D. Williams for persistently encouraging me to perform this study and to D.B. Dougherty for many helpful discussions along the way. I also benefitted greatly from insightful comments from S.V. Khare and F. Szalma.

References

- [1] S.V. Khare, T.L. Einstein, *Phys. Rev. B* 57 (1998) 4782.
- [2] T.L. Einstein, S.V. Khare, in: P.M. Duxbury, T.J. Pence (Eds.), *Dynamics of Crystal Surfaces and Interfaces*, Plenum Press, New York, 1997, p. 83.
- [3] B. Blagojević, P.M. Duxbury, in: P.M. Duxbury, T.J. Pence (Eds.), *Dynamics of Crystal Surfaces and Interfaces*, Plenum Press, New York, 1997, p. 1.
- [4] B. Blagojević, P.M. Duxbury, *Phys. Rev. E* 60 (1999) 1279.
- [5] A. Pimpinelli, J. Villain, D.E. Wolf, J.J. Métois, J.C. Heyraud, I. Elkinani, G. Uimin, *Surf. Sci.* 295 (1993) 143.
- [6] T. Ihle, C. Misbah, O. Pierre-Louis, *Phys. Rev. B* 58 (1998) 2289.
- [7] N.C. Bartelt, T.L. Einstein, E.D. Williams, *Surf. Sci.* 312 (1994) 411.
- [8] M. Giesen, S. Baier, *J. Phys.: Cond. Matt.* 13 (2001) 5009.
- [9] H.-C. Jeong, E.D. Williams, *Surf. Sci. Rep.* 34 (1999) 171.
- [10] M. Giesen, *Prog. Surf. Sci.* 68 (2001) 1.
- [11] A. Pimpinelli, J. Villain, *Physics of Crystal Growth*, Cambridge University Press, Cambridge, 1998, p. 97.
- [12] I. Lyubinetzky, D.B. Dougherty, T.L. Einstein, E.D. Williams, *Phys. Rev. B* 66 (2002) 085327.
- [13] T.L. Einstein, S.V. Khare, M.R. D'Orsogna, O. Pierre-Louis, *Bull. Am. Phys. Soc.* 43 (1998) 110.
- [14] I.S. Gradshteyn, I.M. Ryzhik, *Table of Integrals Series and Products*, Academic Press, San Diego, 1980, p. 930ff., 940ff.